Hindawi
Journal of Optimization
Volume 2019, Article ID 9705792, 19 pages
https://doi.org/10.1155/2019/9705792

Research Article

Optimum Design and Performance Analyses of Convective-Radiative Cooling Fin under the Influence of Magnetic Field Using Finite Element Method

M. G. Sobamowo

Department of Mechanical Engineering, University of Lagos, Akoka, Lagos, Nigeria

Correspondence should be addressed to M. G. Sobamowo; mikegbeminiyi@gmail.com

Received 31 May 2018; Accepted 15 January 2019; Published 17 February 2019

Academic Editor: Liwei Zhang

In this study, the optimum design dimensions and performance analyses of convective-radiative cooling fin subjected to magnetic field are presented using finite element method. The numerical solutions are verified by the exact analytical solution for the linearized models using Laplace transform. The optimum dimensions for the optimum performance of the convection-radiative fin with variable thermal conductivity are investigated and presented graphically. Also, the effects of convective, radiative, and magnetic parameters as well as Biot number on the thermal performance of the cooling fin are analyzed using the numerical solutions. From the results, it is established that the optimum length of the fin and the thermogeometric parameter increases as the nonlinear thermal conductivity term increases. Further analyses also reveal that as the Biot number, convective, radiative, and magnetic parameters, increases, the rate of heat transfer from the fin increases and consequently improves the efficiency of the fin. Additionally, effects of the thermal stability values for the various multiboiling heat transfer modes are established. It is established that, in order to ensure stability and avoid numerical diffusion of the solution by the Galerkin finite element method, the thermogeometric parameter must not exceed some certain values for the different multiboiling heat transfer modes. It is hope that the present study will enhance the understanding of thermal response of solid fin under various factors and fin design considerations.

1. Introduction

The continuous productions of high performance thermal equipment due to the growing demands for the thermal systems require the development of enhanced heat transfer devices for the effective performance and thermal management of the equipment. Moreover, the excessive heat leads to thermal-induced failure in the thermal systems which necessitate the use of fins for heat transfer enhancement. The applications of extended surfaces in thermal systems, electronic and microelectronics components, high-power semiconductor devices, high-power lasers, light emitting diodes (LEDs), computer cooling, sensitive devices, etc. have attracted various research interests in past decades. The thermal analysis of the extended surface involves the development of thermal models for various operating conditions. Different analytical (exact and approximate) and numerical methods have been employed by various researchers to analyze the thermal performance of the extended surfaces under different conditions. Although, different exact analytical methods have been employed [2–8], they are based on the assumptions of constant thermal properties. Indubitably, the idealization of a uniform or constant heat transfer coefficient is not realistic. This is because in practice, heat transfer coefficients have significantly greater values at the fin tip than more than the fin base. Also, the thermal property is temperature-dependent. Such variation of the heat transfer coefficient as a function of temperature is often governed by a power law. Moreover, the thermal conductivity of the fin is also temperature-dependent. Under these circumstances, the differential equations governing the thermal response of the fin become strictly nonlinear. The development of exact analytical solutions for such nonlinear models is very difficult. Consequently, some of the past studies have developed approximate analytical solution in terms of series solutions for the thermal analyses of fins using different approximate

analytical methods [9–28]. Nevertheless, the series solutions involve large number of terms. In practice, such huge expressions are not convenient for use by designers and engineers. Therefore, over the years, various numerical methods have been applied for thermal analysis of various extended surfaces [29–44].

It should be noted that most of the above studies are based on steady state analysis of fin. The transient response of fins is important in a wide range of engineering devices, automobiles, and industrial sectors. In fact, an accurate transient analysis provides insight into the design of fins that would fail in steady state operations but are sufficient for desired operating periods. Consequently, transient analysis of the extended surfaces has been investigated [45–66]. However, they are established on the assumption of fins with insulated tips. Although the effects of tip conditions have been analyzed in the past studies [67–72], they are based on steady stated heat transfer.

The determinations of the optimum dimension of fins have been one of the central focus in the study of effective performance and applications of the extended surfaces. Consequently, some past studies have focused on determining the optimum dimensions and performance of fins operating under different conditions. On such optimization studies, Hrymak [73] presented a combined analysis and optimization of extended heat transfer surfaces while Sonn and Bar-Cohen [74] analyzed optimum cylindrical of pin fin. Razelos and Imre [75] carried out a study on minimum mass convective fins with variable heat transfer coefficients. The authors [76] also investigated the optimum dimensions of circular fins with variable thermal parameters. Pitchumani and Shenoy [77] submitted a unified approach to determining optimum shapes for cooling fins of various geometries. Bhargava and Duffin [78] applied the nonlinear method of Wilkins for cooling fin optimization. Wilkins [79] determined the minimum mass of thin fins which transfer heat only by radiation to surroundings at absolute zero. Razelos [80] investigated the optimum dimensions of convective pin fins with internal heat generation. Maday [81] explored the minimum weight of one-dimensional straight fin. Laor and Kalman [82] studied the performance and optimum dimensions of different cooling fins with a temperature-dependent heat transfer coefficient. Effects of magnetic field and radiative heat transfer on the extended surfaces under steady state conditions have considered in literature [1, 83–86]. Ma et al. [87] adopted spectral collocation method for transient thermal analysis of coupled conductive, convective, and radiative heat transfer in the moving plate with temperature-dependent properties and heat generation. In another work, with the aid of spectral element method, Ma et al. [88] studied the combined conductive, convective, and radiative heat transfer in moving irregular porous fins. Chen et al. [89] utilized least square spectral collocation method to examine the nonlinear heat transfer in moving porous plate with convective and radiative boundary conditions.

The past studies have been based on the optimum analysis of fin under steady state. To the best of the authors' knowledge, the transient analysis and optimum design analysis of heat transfers in convective-radiative cooling fin with convective tip under the influence of magnetic field using finite element method have not been studied in open literature. Therefore, in this present study, finite element method is used to determine the optimum dimension and study the transient thermal behaviour of convective-radiative fin with convective tip and under the influence of magnetic field is analyzed. The numerical solutions are used to investigate of thermogeometric parameter and nonlinear thermal conductivity on the optimum performance of the fin. Also, effects of convective, radiative, magnetic, and convective tip parameters on the transient thermal performance of the cooling fin are investigated. Additionally, effects the thermal stability values for the various multiboiling heat transfer modes are established.

2. Problem Formulation

Consider a straight fin of length L and thickness t which is exposed on both faces to a convective-radiative environment at temperature T_∞ and subjected to a uniform magnetic field as shown in Figure 1. In order to develop the mathematical model governing the thermal behaviour, the following assumptions are made:

(i) The fin material is homogeneous and isotropic and with constant physical properties.

(ii) The thermal properties of the surrounding medium and the magnetic field vary with temperature according to the power law.

(iii) The temperature of the surrounding fluid and the temperature of the base of the fin are uniform.

(iv) The temperature variation inside the fin is one-dimensional. This is because the fin thickness is so small compared to its height that temperature gradients normal to the surface may be neglected.

(v) Heat loss through the fin edges is negligible compared to that which passes through the sides.

(vi) There is no contact resistance where the base of the fin joins the prime surface. Also, the specific heat capacity of the fin is constant.

(vii) There are no heat sources or internal heat generation within the fin.

From the energy balance analysis based on the assumptions stated above, the thermal energy balance could be expressed as

$$q_x - \left(q_x + \frac{\delta q}{\delta x}dx\right) = h(T)\,P\left(T - T_\infty\right)dx + \sigma\varepsilon(T)\,P\left(T^4 - T_\infty^4\right)dx + \frac{\mathbf{J_c}\times\mathbf{J_c}}{\sigma_m}dx + \rho A_{cr}c_p\frac{\partial T}{\partial t}dx \quad (1)$$

where Jc is the conduction current intensity and is given as

$$\mathbf{J_c} = \sigma_m\left(\mathbf{E} + \mathbf{V}\times\mathbf{B}\right) \quad (2)$$

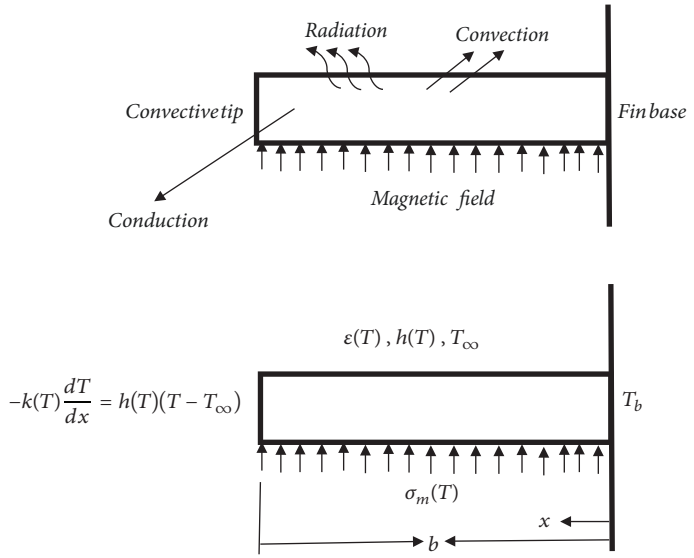

Figure 1: (a) Schematic of longitudinal fin subjected to magnetic field [1]. (b) Computational domain of the fin [1].

After expansion and simplification of the above equation, using the fact that as $dx \longrightarrow 0$, then (1) reduces

$$-\frac{dq}{dx} = h(T)\,P\left(T - T_a\right) + \sigma\varepsilon(T)\,P\left(T^4 - T_a^4\right) + \frac{\mathbf{J_c} \times \mathbf{J_c}}{\sigma_m} + \rho A_{cr} c_p \frac{\partial T}{\partial t} \tag{3}$$

According to Fourier's law of heat conduction, the rate of heat conduction in the fin is given by

$$q = -k(T)\,A_{cr}\frac{dT}{dx} \tag{4}$$

while the radiation heat transfer rate is given as

$$q = -\frac{4\sigma A_{cr}}{3\beta_R}\frac{dT^4}{dx} \tag{5}$$

From (4) and (5), it could be stated that the total rate of heat transfer is given by

$$q = -k(T)\,A_{cr}\frac{dT}{dx} - \frac{4\sigma A_{cr}}{3\beta_R}\frac{dT^4}{dx} \tag{6}$$

If one substitutes (6) into (3), one arrives at

$$\frac{d}{dx}\left(k(T)\,A_{cr}\frac{dT}{dx} + \frac{4\sigma A_{cr}}{3\beta_R}\frac{dT^4}{dx}\right) = h(T)\,P\left(T - T_\infty\right) + \sigma(T)\,\varepsilon P\left(T^4 - T_\infty^4\right) + \frac{\mathbf{J_c} \times \mathbf{J_c}}{\sigma_m} + \rho A_{cr} c_p \frac{\partial T}{\partial t} \tag{7}$$

A further simplification of (7) gives the governing differential equation for the fin as

$$\frac{d}{dx}\left(k(T)\frac{dT}{dx}\right) + \frac{4\sigma}{3\beta_R}\frac{d}{dx}\left(\frac{dT^4}{dx}\right) - \frac{h(T)\,P}{A_{cr}}\left(T - T_\infty\right) - \frac{\sigma\varepsilon(T)\,P}{A_{cr}}\left(T^4 - T_\infty^4\right) - \frac{\mathbf{J_c} \times \mathbf{J_c}}{\sigma_m A_{cr}} = \rho c_p \frac{\partial T}{\partial t} \tag{8}$$

The initial and boundary conditions are

$$\begin{aligned} &t = 0,\ 0 < x < b,\ T = T_b \\ &t > 0,\ x = 0,\ T = T_b \\ &t > 0,\ x = b,\ -k\frac{dT}{dx} = h\left(T - T_\infty\right) \end{aligned} \tag{9}$$

However, if the tip of the fin is assumed insulated or a negligible rate of heat transfer from it, we have

$$t > 0,\ x = b,\ \frac{dT}{dx} = 0 \tag{10}$$

It should be noted that

$$\frac{\mathbf{J_c} \times \mathbf{J_c}}{\sigma} = \sigma_m B_o^2 u^2 \tag{11}$$

After substitution of (11) into (8),

$$\frac{d}{dx}\left(k(T)\frac{dT}{dx}\right) + \frac{4\sigma}{3\beta_R}\frac{d}{dx}\left(\frac{dT^4}{dx}\right) - \frac{h(T)\,P}{A_{cr}}\left(T - T_\infty\right) - \frac{\sigma\varepsilon(T)\,P}{A_{cr}}\left(T^4 - T_\infty^4\right) - \frac{\sigma_m(T)\,B_o^2 u^2}{A_{cr}}\left(T - T_\infty\right) = \rho c_p \frac{\partial T}{\partial t} \tag{12}$$

If a small temperature difference exists within the fin material during the heat flow, the term T^4 can be expressed as a linear function of temperature as

$$T^4 = T_\infty^4 + 4T_\infty^3 (T - T_\infty) + 6T_\infty^2 (T - T_\infty)^2 + \cdots \cong 4T_\infty^3 T - 3T_\infty^4 \quad (13)$$

Also, with the aid of Rosseland's approximation, one can express the nonlinear derivative term in (12) as

$$\frac{4\sigma}{3\beta_R k}\frac{\partial T^4}{\partial x} \cong \frac{16\sigma T_\infty^3}{3\beta_R k}\frac{\partial^2 T}{\partial x^2} \quad (14)$$

If one substitutes (13) and (14) into (12), we arrive at

$$\frac{d}{dx}\left(k(T)\frac{dT}{dx}\right) + \frac{16\sigma}{3\beta_R}\frac{d^2T}{dx^2} - \frac{h(T)P}{A_{cr}}(T - T_\infty) - \frac{4\sigma P\varepsilon(T)T_\infty^3}{A_{cr}}(T - T_\infty) - \frac{\sigma_m(T)B_o^2u^2}{A_{cr}}(T - T_\infty) = \rho c_p\frac{\partial T}{\partial t} \quad (15)$$

where

$$k(T) = k_a(1 + \beta(T - T_\infty)) \quad (16)$$

For most industrial applications the heat transfer coefficient may be given as the power law [3, 20], where the exponents p and h_o are constants. The constant n may vary between −6.6 and 5. However, in most practical applications it lies between −3 and 3 [20]. So, the power temperature-dependent thermal properties of the surrounding fluid and the magnetic field are defined as

$$h(T) = h_o\left(\frac{T - T_\infty}{T_b - T_\infty}\right)^p \quad (17)$$

Extending the same power temperature-dependent relationship to the fin emissivity and the magnetic field, we have

$$\varepsilon(T) = \varepsilon_o\left(\frac{T - T_\infty}{T_b - T_\infty}\right)^q \quad (18)$$

$$\sigma_m(T) = (\sigma_m)_o\left(\frac{T - T_\infty}{T_b - T_\infty}\right)^r \quad (19)$$

The exponent p on the heat transfer coefficient represents laminar film boiling or condensation when $p = -1/4$, laminar natural convection when $p = 1/4$, turbulent natural convection when $p = 1/3$, nucleate boiling when $p = 2$, and radiation when $p = 3$. $p = 0$ implies a constant heat transfer coefficient.

Substitution of (17)-(19) gives

$$\frac{d}{dx}\left(k(T)\frac{dT}{dx}\right) + \frac{16\sigma}{3\beta_R}\frac{d^2T}{dx^2} - \frac{h_oP(T - T_\infty)^{p+1}}{A_{cr}(T_b - T_\infty)^p} - \frac{4\sigma\varepsilon_oPT_\infty^3(T - T_\infty)^{q+1}}{A_{cr}(T_b - T_\infty)^q} - \frac{\sigma_{m,o}B_o^2u^2(T - T_\infty)^{r+1}}{A_{cr}(T_b - T_\infty)^r} = \rho c_p\frac{\partial T}{\partial t} \quad (20)$$

3. Finite Element Method for the Transient Analysis

It is very difficult to develop exact analytical solution to the nonlinear equation in (15) or (20). Therefore, Galerkin finite element method is used in this work to solve the nonlinear equation. Using the shape/interpolating function on the governing equation and Integrating over the domain V of the control volume according to Galerkin finite element method, we have

$$\int_V W\left(\frac{d}{dx}\left(k(T)\frac{dT}{dx}\right) + \left(\frac{16\sigma}{3\beta_R}\frac{d^2T}{dx^2}\right) - \left(\frac{\left(hP(T) + 4\sigma P(T)\varepsilon_oT_\infty^3 + \sigma_m(T)B_o^2u^2\right)}{A_{cr}}\right) \cdot (T - T_\infty) - \rho c_p\frac{\partial T}{\partial t} = 0\right)dV = 0 \quad (21)$$

For the one-dimensional problem of which the dependent variable varies only along x-axis and the boundary integrals turn to be a point value on boundaries, one can replace dV by $A_{cr}dx$ in (21). Here, A_{cr} is the uniform cross-sectional area of the fin and P is the perimeter of the fin from which convection takes place.

$$\int_L W\left(\frac{d}{dx}\left(k(T)\frac{dT}{dx}\right) + \left(\frac{16\sigma}{3\beta_R}\frac{d^2T}{dx^2}\right) - \left(\frac{\left(hP(T) + 4\sigma P(T)\varepsilon_oT_\infty^3 + \sigma_m(T)B_o^2u^2\right)}{A_{cr}}\right) \cdot (T - T_\infty) - \rho c_p\frac{\partial T}{\partial t} = 0\right)A_{cr}dx = 0 \quad (22)$$

$$\int_0^L \rho c_pA_{cr}W\frac{\partial T}{\partial t}dx + \int_0^L A_{cr}\frac{\partial W}{\partial x}k(T)\frac{\partial T}{\partial x} + \int_0^L\left(\frac{16\sigma}{3\beta_R}\right)A_{cr}\frac{\partial W}{\partial x}\frac{\partial T}{\partial x}dx + \int_0^L\left(h(T) + 4\sigma(T)\cdot\varepsilon_oT_\infty^3\right)PWT\,dx + \int_0^L\sigma_m(T)B_o^2u^2WT\,dx = \int_0^L\left(h(T) + 4\sigma(T)\varepsilon_oT_\infty^3\right)PT_\infty W\,dx + \int_0^L\sigma_m(T)B_o^2u^2WT_\infty dx + A_{cr}\left(\frac{16\sigma}{3\beta_R}\right)\frac{\partial T}{\partial x}\Big|_0^L W + A_{cr}\,k(T)\frac{\partial T}{\partial x}\Big|_0^L W \quad (23)$$

Equation (23) is a weak formulation of the nonlinear governing differential equation.

Following the usual finite element procedures, the analysis of (23) gives

$$\begin{aligned}
&\int_0^{L_e} \rho c_p A_{cr} [\mathbf{W}]^T [\mathbf{W}] \left\{\frac{\partial \mathbf{T}}{\partial t}\right\} dx \\
&\quad + \int_0^{L_e} k(T) A_{cr} [\mathbf{B}]^T [\mathbf{B}] [\mathbf{T}] dx \\
&\quad + \int_0^{L_e} \left(\frac{16\sigma}{3\beta_R}\right) A_{cr} [\mathbf{B}]^T [\mathbf{B}] [\mathbf{T}] dx \\
&\quad + \int_0^{L_e} \left(h(T) + 4\sigma(T)\varepsilon_o T_\infty^3\right) P [\mathbf{W}]^T [\mathbf{W}] [\mathbf{T}] dx \\
&\quad + \int_0^{L_e} \sigma_m(T) B_o^2 u^2 [\mathbf{W}]^T [\mathbf{W}] [\mathbf{T}] dx \\
&= \int_0^{L_e} \left(h(T) + 4\sigma(T)\varepsilon_o T_\infty^3\right) P [\mathbf{W}]^T T_\infty dx \\
&\quad + \left(A_{cr}\left(\frac{16\sigma}{3\beta_R}\right)\frac{\partial T}{\partial x}\right)\Bigg|_0^{L_e} [\mathbf{W}]^T \\
&\quad + \left(A_{cr} k(T) \frac{\partial T}{\partial x}\right)\Bigg|_0^{L_e} [\mathbf{W}]^T
\end{aligned} \tag{24}$$

Equation (24) can be written form as

$$[\mathbf{C}] \left\{\frac{\partial \mathbf{T}}{\partial t}\right\} + [\mathbf{K}(T)] \{\mathbf{T}\} = [\mathbf{f}(T)] \tag{25}$$

where

$$[\mathbf{C}] = \int_0^{L_e} \rho c_p A [\mathbf{W}]^T [\mathbf{W}] dx \tag{26}$$

$$\begin{aligned}
&[\mathbf{K}(T)] \\
&= + \int_0^{L_e} k(T) A_{cr} [\mathbf{B}]^T [\mathbf{B}] [\mathbf{T}] dx \\
&\quad + \int_0^{L_e} \left(\frac{16\sigma}{3\beta_R}\right) A_{cr} [\mathbf{B}]^T [\mathbf{B}] [\mathbf{T}] dx \\
&\quad + \int_0^{L_e} \left(h(T) + 4\sigma(T)\varepsilon_o T_\infty^3\right) P [\mathbf{W}]^T [\mathbf{W}] dx \\
&\quad + \int_0^{L_e} \sigma_m(T) B_o^2 u^2 [\mathbf{W}]^T [\mathbf{W}] dx
\end{aligned} \tag{27}$$

$$\begin{aligned}
&[\mathbf{f}(T)] \\
&= \int_0^{L_e} \left(h(T) + 4\sigma(T)\varepsilon_o T_\infty^3\right) P T_\infty [\mathbf{W}]^T T_\infty dx \\
&\quad + \int_0^{L_e} \sigma_m(T) B_o^2 u^2 T_\infty [\mathbf{W}]^T T_\infty dx \\
&\quad + \left(A_{cr}\left(\frac{16\sigma}{3\beta_R}\right)\frac{\partial T}{\partial x}\right)\Bigg|_0^{L_e} [\mathbf{W}]^T \\
&\quad + \left(A_{cr} k(T) \frac{\partial T}{\partial x}\right)\Bigg|_0^{L_e} [\mathbf{W}]^T
\end{aligned} \tag{28}$$

and

$$[\mathbf{W}] = [W_i \;\; W_j] \tag{29}$$

is the shape function matrix and

$$\{\mathbf{T}\} = \begin{bmatrix} T_i \\ T_j \end{bmatrix} \tag{30}$$

is the vector of unknown temperatures

$$[\mathbf{B}] = \begin{bmatrix} \frac{\partial W_i}{\partial x} & \frac{\partial W_j}{\partial x} \end{bmatrix} \tag{31}$$

Using a 3-node element as shown in Figure 2, one arrives at

$$\left[C_{ij}\right] = \frac{\rho c_p A_{cr} L_e}{6} \begin{bmatrix} 8 & 4 & -2 \\ 4 & 32 & 4 \\ -2 & 4 & 8 \end{bmatrix} \tag{32}$$

$$\begin{aligned}
\left[K_{ij}(T)\right] &= \left[\frac{\left(k(T) + 16\sigma/3\beta_R\right) A_{cr}}{3L_e} \begin{bmatrix} 7 & -8 & 1 \\ -8 & 16 & -8 \\ 1 & -8 & 7 \end{bmatrix}\right. \\
&\quad + \left(h(T) P + 4\sigma(T)\varepsilon_o T_\infty^3 P + \sigma_m(T) B_o^2 u^2\right) \frac{L_e}{60} \\
&\quad \left. \cdot \begin{bmatrix} 8 & 4 & -2 \\ 4 & 32 & 4 \\ -2 & 4 & 8 \end{bmatrix}\right]
\end{aligned} \tag{33}$$

$$\begin{aligned}
\left[f_i(T)\right] &= \left(h(T) P + 4\sigma(T)\varepsilon_o T_\infty^3 P + \sigma_m(T) B_o^2 u^2\right) \\
&\quad \cdot \frac{T_\infty L_e}{6} \begin{bmatrix} 1 \\ 4 \\ 1 \end{bmatrix} + \left(k(\mathrm{T}) + \frac{16\sigma}{3\beta_R}\right) A_{cr} \begin{bmatrix} -\frac{\partial T(0)}{\partial x} \\ \frac{\partial T(M)}{\partial x} \\ \frac{\partial T(L)}{\partial x} \end{bmatrix}
\end{aligned} \tag{34}$$

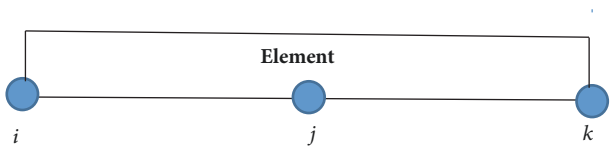

Figure 2: A 3-node element.

After the substitution of (32)-(34), we arrived at

$$\frac{\rho c_p A_{cr} L_e}{6}\begin{bmatrix} 8 & 4 & -2 \\ 4 & 32 & 4 \\ -2 & 4 & 8 \end{bmatrix}\begin{Bmatrix} \frac{\partial T_i}{\partial t} \\ \frac{\partial T_j}{\partial t} \\ \frac{\partial T_k}{\partial t} \end{Bmatrix} + \left[\frac{\left(k\left(T\right)+16\sigma/3\beta_R\right)A_{cr}}{3L_e}\begin{bmatrix} 7 & -8 & 1 \\ -8 & 16 & -8 \\ 1 & -8 & 7 \end{bmatrix} + \left(h\left(T\right)P + 4\sigma\left(T\right)\varepsilon_o T_\infty^3 P + \sigma_m\left(T\right)B_o^2 u^2\right)\frac{L_e}{60} \cdot \begin{bmatrix} 8 & 4 & -2 \\ 4 & 32 & 4 \\ -2 & 4 & 8 \end{bmatrix}\right]\begin{Bmatrix} T_i \\ T_j \\ T_k \end{Bmatrix} = \left(h\left(T\right)P + 4\sigma\left(T\right)\varepsilon_o T_\infty^3 P + \sigma_m\left(T\right)B_o^2 u^2\right)\frac{T_\infty L_e}{6}\begin{bmatrix} 1 \\ 4 \\ 1 \end{bmatrix} + \left(k\left(T\right) + \frac{16\sigma}{3\beta_R}\right)A_{cr}\begin{bmatrix} -\frac{\partial T\left(0\right)}{\partial x} \\ \frac{\partial T\left(M\right)}{\partial x} \\ \frac{\partial T\left(L\right)}{\partial x} \end{bmatrix} \tag{35}$$

3.1. Time Discretization Using the Finite Element Method. The above equation is a general representation of a one-dimensional problem with one linear element. All the terms are included irrespective of the boundary condition. Equation (25) is semidiscrete as it is discretized only in space. The differential operator still contains the time-dependent term and it has to be discretized. We now require a method of discretizing the transient terms of the equation. The following subsections give the details of how the transient terms will be discretized. In (25), the temperature is now discretized in the time domain as in Figure 2.

Using Figure 3,

$$\begin{aligned} T\left(t\right) &= N_i\left(t\right)T_i\left(t\right) + N_j\left(t\right)T_j\left(t\right) \\ &= \begin{bmatrix} N_i\left(t\right) & N_j\left(t\right) \end{bmatrix}\begin{Bmatrix} T_i\left(t\right) \\ T_j\left(t\right) \end{Bmatrix}. \end{aligned} \tag{36}$$

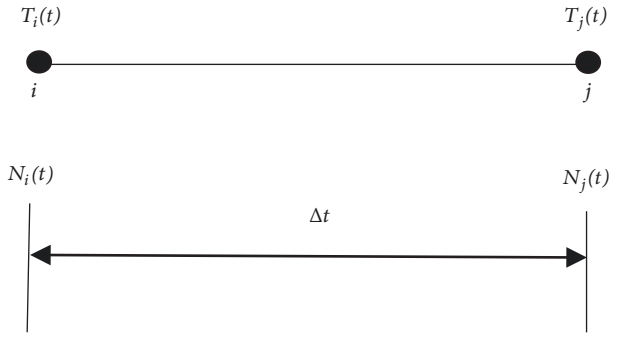

Figure 3: Time discretization between nth (i) and $n+1$th (j) time levels.

Following the similar procedure as done previously, we can derive the linear shape functions as

$$\begin{aligned} N_i\left(t\right) &= 1 - \frac{t}{\Delta t}, \\ N_j\left(t\right) &= \frac{t}{\Delta t}. \end{aligned} \tag{37}$$

Therefore, the time derivative of the temperature is thus written as

$$\begin{aligned} \frac{\partial T\left(t\right)}{\partial t} &= \frac{\partial N_i\left(t\right)}{\partial t}T_i\left(t\right) + \frac{\partial N_j\left(t\right)}{\partial t}T_j\left(t\right) \\ &= \left(-\frac{1}{\Delta t}\right)T_i\left(t\right) + \left(\frac{1}{\Delta t}\right)T_j\left(t\right) \\ &= \frac{1}{\Delta t}\left(T_j\left(t\right) - T_i\left(t\right)\right) \Longrightarrow \\ \frac{\partial T\left(t\right)}{\partial t} &= \begin{bmatrix} -\frac{1}{\Delta t} & \frac{1}{\Delta t} \end{bmatrix}\begin{Bmatrix} T_i\left(t\right) \\ T_j\left(t\right) \end{Bmatrix} \end{aligned} \tag{38}$$

Substituting (36) and (37) into (25) and applying the weighted residual principle (Galerkin method), we obtain for a time interval of Δt,

$$\int_{\Delta t}\left[\begin{bmatrix} N_i\left(t\right) \\ N_j\left(t\right) \end{bmatrix}\left[\left[\mathbf{C}\right]\begin{bmatrix} -\frac{1}{\Delta t} & \frac{1}{\Delta t} \end{bmatrix}\begin{Bmatrix} T_i\left(t\right) \\ T_j\left(t\right) \end{Bmatrix} + \left[\mathbf{K}\left(T\right)\right]\begin{bmatrix} N_i\left(t\right) & N_j\left(t\right) \end{bmatrix}\begin{Bmatrix} T_i\left(t\right) \\ T_j\left(t\right) \end{Bmatrix} - \left[\mathbf{f}\left(T\right)\right]\right]\right]dt \tag{39}$$

After expansion

$$\int_{\Delta t}\left[\left[[\mathbf{C}]\begin{bmatrix}N_i(t)\\N_j(t)\end{bmatrix}\left[-\frac{1}{\Delta t}\quad\frac{1}{\Delta t}\right]\begin{Bmatrix}T_i(t)\\T_j(t)\end{Bmatrix}+[\mathbf{K}(T)]\begin{bmatrix}N_i(t)\\N_j(t)\end{bmatrix}\left[N_i(t)\quad N_j(t)\right]\begin{Bmatrix}T_i(t)\\T_j(t)\end{Bmatrix}-\begin{bmatrix}N_i(t)\\N_j(t)\end{bmatrix}[\mathbf{f}(T)]\right]\right]dt \tag{40}$$

Substituting (37) into (40)

$$\int_{\Delta t}\left[\left[[\mathbf{C}]\begin{bmatrix}1-\frac{t}{\Delta t}\\\frac{t}{\Delta t}\end{bmatrix}\left[-\frac{1}{\Delta t}\quad\frac{1}{\Delta t}\right]\begin{Bmatrix}T_i(t)\\T_j(t)\end{Bmatrix}+[\mathbf{K}(T)]\begin{bmatrix}1-\frac{t}{\Delta t}\\\frac{t}{\Delta t}\end{bmatrix}\left[1-\frac{t}{\Delta t}\quad\frac{t}{\Delta t}\right]\begin{Bmatrix}T_i(t)\\T_j(t)\end{Bmatrix}-\begin{bmatrix}1-\frac{t}{\Delta t}\\\frac{t}{\Delta t}\end{bmatrix}[\mathbf{f}(T)]\right]\right]dt \tag{41}$$

Again, after expansion of (41), one arrives at

$$\int_{\Delta t}\left[\left[[\mathbf{C}]\cdot\begin{bmatrix}-\left(1-\frac{t}{\Delta t}\right)\left(\frac{1}{\Delta t}\right) & \left(1-\frac{t}{\Delta t}\right)\left(\frac{1}{\Delta t}\right)\\-\left(\frac{t}{\Delta t}\right)\left(\frac{1}{\Delta t}\right) & \left(\frac{t}{\Delta t}\right)\left(\frac{1}{\Delta t}\right)\end{bmatrix}\begin{Bmatrix}T_i(t)\\T_j(t)\end{Bmatrix}+[\mathbf{K}(T)]\cdot\begin{bmatrix}\left(1-\frac{t}{\Delta t}\right)^2 & \left(1-\frac{t}{\Delta t}\right)\left(\frac{t}{\Delta t}\right)\\\left(1-\frac{t}{\Delta t}\right)\left(\frac{t}{\Delta t}\right) & \left(\frac{t}{\Delta t}\right)^2\end{bmatrix}\begin{Bmatrix}T_i(t)\\T_j(t)\end{Bmatrix}-\begin{bmatrix}1-\frac{t}{\Delta t}\\\frac{t}{\Delta t}\end{bmatrix}[\mathbf{f}(T)]\right]\right]dt \tag{42}$$

After the evaluation of (40), we obtained the characteristic equation over the time interval Δt as

$$\frac{1}{2\Delta t}\left[[\mathbf{C}]\begin{bmatrix}-1 & 1\\-1 & 1\end{bmatrix}\begin{Bmatrix}T_i(t)\\T_j(t)\end{Bmatrix}+\frac{1}{3}[\mathbf{K}(T)]\begin{bmatrix}2 & 1\\1 & 2\end{bmatrix}\begin{Bmatrix}T_i(t)\\T_j(t)\end{Bmatrix}=\frac{1}{2}\begin{bmatrix}1\\1\end{bmatrix}\begin{Bmatrix}f_1\\f_2\end{Bmatrix}\right] \tag{43}$$

The above equation involves the temperature values at the *nth* and $(n+1)th$ level. The boundary conditions and the temperature-dependent parameters are incorporated in the computer program used to solve the system of differential equations. Although a dimensionless form of the governing equation can be derived for the computer program, the handling of physical quantities is simplified. It should be noted that the thermal properties are evaluated directly in each time step from the nodal temperatures. This eliminates any iteration within each time step for the evaluations of the temperature-dependent parameters.

The element equation/matrix has been derived as shown in the previous equations. It should be noted that the whole domain was divided into a set of 50 line elements. Assembling all the elements equation/matrices, a global matrix or a system of equations was obtained. After applying the boundary conditions, the resulting systems of equations are solved numerically. The convergence criterion of the numerical solution along with error estimation has been set to

$$\sum_{i}^{N}\left|\phi_i^i-\phi^{i-1}\right|\le 10^{-4} \tag{44}$$

where φ is the general dependent variable T and i is the number of iteration.

It should be noted that a steady state is attained when $\partial T/\partial t = 0$ or $t \longrightarrow \infty$.

4. Optimization of the Longitudinal Fin

The fin weight and material costs are the primary design considerations in most applications of fin. Therefore, it is highly desirable to obtain the optimum design information of fins.

The optimization of the fin could be achieved either by minimizing the volume (weight) for any required heat dissipation or by maximizing the heat dissipation for any given fin volume [73–76]. The later approach is adopted in this work.

The constant fin volume is defined as $V=A_c w$. We can therefore write the heat dissipation per unit volume as

$$\frac{q_f}{V}=\frac{\int_0^L Ph\,(T-T_\infty)\,dx}{A_c w} \tag{45}$$

The dimensionless form of (45) is given as

$$Q_f=\frac{q_f}{k\,(\mathrm{T}_b-\mathrm{T}_\infty)}\left(\frac{A_p}{V}\right)=\frac{A_p}{k\,(\mathrm{T}_b-\mathrm{T}_\infty)}\frac{\int_0^L Ph\,(T-T_\infty)\,dx}{A_c w} \tag{46}$$

Equation (46) could be written as

$$Q_f=\frac{\xi M^{2/3}}{(T_b-T_\infty)}\int_0^1 (T-T_\infty)\,dx \tag{47}$$

where

$$M = \left(\frac{hP}{kA_c}\right)^{0.5},$$
$$\xi = \left(\frac{2h\sqrt{A_p}}{k}\right)^{2/3}, \quad (48)$$
$$A_p = \delta w$$

The maximum heat dissipation value occurs at the condition when the optimum fin characteristics have been achieved. The fin dimensions in this situation represent the optimum fin configuration per unit volume. With the volume constant, the optimization procedure is also carried out to fix the profile area A_p by first expressing Q_f/ξ as a function of the thermogeometric parameter, M (or fin length, b) and then searching for the optimum value of M [73–76] where $d(Q_f/\xi)/dM = 0$.

5. Development of an Exact Analytical Solution for the Verification of the Numerical Solution

For constant thermal properties of the surrounding fluid and the magnetic field, we have a linear equation of the form

$$\frac{d^2T}{dx^2} + \frac{16\sigma}{3\beta_R}\frac{d^2T}{dx^2} - \frac{hP\left(T - T_\infty\right)}{kA_{cr}} - \frac{4\sigma\varepsilon PT_\infty^3\left(T - T_\infty\right)}{kA_{cr}} - \frac{\sigma_m B_o^2 u^2\left(T - T_\infty\right)}{kA_{cr}} = \frac{\rho c_p}{k}\frac{\partial T}{\partial t} \quad (49)$$

It should be noted that (49) can be solved analytically. Using Laplace transform, it can easily be shown that the exact analytical solution of the equation based on the initial and the boundary conditions in (9) is given as

$$T = T_\infty + (T_b - T_\infty) \cdot \left\{ \frac{\left(\left(hP + 4\sigma\varepsilon T_\infty^3 P + \sigma_m B_o^2 u^2\right) L/A_{cr}\left(k + 16\sigma/3\beta_R\right)\right)\cosh\left(\left(hP + 4\sigma\varepsilon T_\infty^3 P + \sigma_m B_o^2 u^2\right)/A_{cr}\left(k + 16\sigma/3\beta_R\right)\right)(L - x) + (hL/k)\sinh\left(\left(hP + 4\sigma\varepsilon T_\infty^3 P + \sigma_m B_o^2 u^2\right)/A_{cr}\left(k + 16\sigma/3\beta_R\right)\right)(L - x)}{\left(\left(hP + 4\sigma\varepsilon T_\infty^3 P + \sigma_m B_o^2 u^2\right) L/A_{cr}\left(k + 16\sigma/3\beta_R\right)\right)\cosh\left(\left(hP + 4\sigma\varepsilon T_\infty^3 P + \sigma_m B_o^2 u^2\right) L/A_{cr}\left(k + 16\sigma/3\beta_R\right)\right) + (hL/k)\sinh\left(\left(\left(hP + 4\sigma\varepsilon T_\infty^3 P + \sigma_m B_o^2 u^2\right) L/A_{cr}\left(k + 16\sigma/3\beta_R\right)\right)\right)} - 2\sum_{n=1}^{\infty}\left\{ \frac{\lambda_n^3 \sin\left(\lambda_n x/L\right)\left\{\exp - \left[\left(\lambda_n^2 + \left(\left(hP + 4\sigma\varepsilon T_\infty^3 P + \sigma_m B_o^2 u^2\right) L/A_{cr}\left(k + 16\sigma/3\beta_R\right)\right)^2\right)\left(\left(k + 16\sigma/3\beta_R\right) t/\rho c_p L^2\right)\right]\right\}}{\left(\lambda_n^2 + \left(\left(hP + 4\sigma\varepsilon T_\infty^3 P + \sigma_m B_o^2 u^2\right) L/A_{cr}\left(k + 16\sigma/3\beta_R\right)\right)^2\right)\left((hL/k)^2 + \left(\left(hP + 4\sigma\varepsilon T_\infty^3 P + \sigma_m B_o^2 u^2\right) L/A_{cr}\left(k + 16\sigma/3\beta_R\right)\right)^2 + hL/k\right)\sin^2\lambda_n} \right\} \right\}. \quad (50)$$

For the insulated tip, we have

$$T = T_\infty + (T_b - T_\infty) \cdot \left\{ \frac{\left(\left(hP + 4\sigma\varepsilon T_\infty^3 P + \sigma_m B_o^2 u^2\right) L/A_{cr}\left(k + 16\sigma/3\beta_R\right)\right)\cosh\left(\left(hP + 4\sigma\varepsilon T_\infty^3 P + \sigma_m B_o^2 u^2\right)/A_{cr}\left(k + 16\sigma/3\beta_R\right)\right)(L - x)}{\left(\left(hP + 4\sigma\varepsilon T_\infty^3 P + \sigma_m B_o^2 u^2\right) L/A_{cr}\left(k + 16\sigma/3\beta_R\right)\right)\cosh\left(\left(hP + 4\sigma\varepsilon T_\infty^3 P + \sigma_m B_o^2 u^2\right) L/A_{cr}\left(k + 16\sigma/3\beta_R\right)\right)} - 2\sum_{n=1}^{\infty}\left\{ \frac{\lambda_n^3 \sin\left(\lambda_n x/L\right)\left\{\exp - \left[\left(\lambda_n^2 + \left(\left(hP + 4\sigma\varepsilon T_\infty^3 P + \sigma_m B_o^2 u^2\right) L/A_{cr}\left(k + 16\sigma/3\beta_R\right)\right)^2\right)\left(\left(k + 16\sigma/3\beta_R\right) t/\rho c_p L^2\right)\right]\right\}}{\left(\lambda_n^2 + \left(\left(hP + 4\sigma\varepsilon T_\infty^3 P + \sigma_m B_o^2 u^2\right) L/A_{cr}\left(k + 16\sigma/3\beta_R\right)\right)^2\right)\left(\left(\left(hP + 4\sigma\varepsilon T_\infty^3 P + \sigma_m B_o^2 u^2\right) L/A_{cr}\left(k + 16\sigma/3\beta_R\right)\right)^2\right)\sin^2\lambda_n} \right\} \right\}. \quad (51)$$

where λ_n are the positive roots of the characteristics equation

$$\lambda_n \cos\lambda_n + \left(\frac{hL}{k}\right)\sin\lambda_n = 0. \quad (52)$$

It should be noted that a steady state is attained when $t \longrightarrow \infty$.

And the steady state solution for the fin with convective tip can be written as

$$T = T_\infty + (T_b - T_\infty) \cdot \left\{ \frac{\left(\left(hP + 4\sigma\varepsilon T_\infty^3 P + \sigma_m B_o^2 u^2\right) L/A_{cr}\left(k + 16\sigma/3\beta_R\right)\right)\cosh\left(\left(hP + 4\sigma\varepsilon T_\infty^3 P + \sigma_m B_o^2 u^2\right)/A_{cr}\left(k + 16\sigma/3\beta_R\right)\right)(L - x) + (hL/k)\sinh\left(\left(hP + 4\sigma\varepsilon T_\infty^3 P + \sigma_m B_o^2 u^2\right)/A_{cr}\left(k + 16\sigma/3\beta_R\right)\right)(L - x)}{\left(\left(hP + 4\sigma\varepsilon T_\infty^3 P + \sigma_m B_o^2 u^2\right) L/A_{cr}\left(k + 16\sigma/3\beta_R\right)\right)\cosh\left(\left(hP + 4\sigma\varepsilon T_\infty^3 P + \sigma_m B_o^2 u^2\right) L/A_{cr}\left(k + 16\sigma/3\beta_R\right)\right) + (hL/k)\sinh\left(\left(\left(hP + 4\sigma\varepsilon T_\infty^3 P + \sigma_m B_o^2 u^2\right) L/A_{cr}\left(k + 16\sigma/3\beta_R\right)\right)\right)} \right\}. \quad (53)$$

Table 1: Thermogeometric parameters used for the simulation.

S/N	Parameter	Value of Parameter
1	Fin thickness (δ)	0.005 m
2	Fin length (L)	0.10 m
3	Specific heat (C)	0.048 kJ/kg°C
4	Density of the fin material (ρ)	7800 kg/m^3
5	Thermal conductivity (k)	12W/m°C
6	Heat transfer coefficient (h_o)	20 W/m^2°C
7	Electrical conductivity (σ_m)	5x10^7 S/m
8	Magnetic field intensity (B_O)	5μT
9	Axial velocity (u)	2.5 m/s
10	power-index, $p = q = r$	0.175
11	Fin base temperature (T_b)	200°C
12	Initial temperature (T_o)	200°C
13	Ambient temperature (T_∞)	30°C
14	Time step (Δt)	10 sec

While, for the fin with insulated tip,

$$T = T_\infty + (T_b - T_\infty) \cdot \left\{ \frac{\left(\left(hP + 4\sigma\varepsilon T_\infty^3 P + \sigma_m B_o^2 u^2\right) L/A_{cr}\left(k + 16\sigma/3\beta_R\right)\right) \cosh\left(\left(hP + 4\sigma\varepsilon T_\infty^3 P + \sigma_m B_o^2 u^2\right)/A_{cr}\left(k + 16\sigma/3\beta_R\right)\right)(L - x)}{\left(\left(hP + 4\sigma\varepsilon T_\infty^3 P + \sigma_m B_o^2 u^2\right) L/A_{cr}\left(k + 16\sigma/3\beta_R\right)\right) \cosh\left(\left(hP + 4\sigma\varepsilon T_\infty^3 P + \sigma_m B_o^2 u^2\right) L/A_{cr}\left(k + 16\sigma/3\beta_R\right)\right)} \right\}. \quad (54)$$

For the sake of convenience in subsequent analysis, it should be noted that "b" has been replaced with "L" in the above analytical solution.

Table 1 shows the thermogeometric parameters used for the simulation.

6. Results and Discussion

For the computational domain, numerical solutions are computed and the necessary convergence of the results is achieved with the desired degree of accuracy. Using the numerical solutions, parametric studies are carried out. Also, in order to define the validity of the results of thermal analysis of fin with assumed insulated tip and that of convective tip, effects of the fin tip conditions on the transient thermal response are investigated. The results with the discussion are illustrated through the Figures 4–16 and Table 2 to substantiate the applicability of the present analysis.

In order to verify the accuracy of the present numerical method, the numerical results are compared with results obtained by exact analytical method for the linearized equation (Table 2). It is inferred from the figure that there are excellent agreements between the FEM results and the analytical results, which testifies to the validity of the FEM code. This validation boosts the confidence in the numerical outcome of the present study. Moreover, it is observed that, in the same domain by increasing the polynomial degree of approximation or the number of nodes in an element, one can achieve the desired accuracy with less DOF.

Table 2 shows the comparison of the results obtained by exact analytical and finite element methods for a conductive-convective fin with constant thermal and physical properties of fin having negligible radiation and magnetic field effects. Very good agreements are found between the exact analytical and finite element solutions. The average percentage error of the numerical solution is 0.133%.

Figure 4 shows the nondimensional heat transfer Q/ζ (for a unit fin volume) varying with M from 1 and 2 for specified values of nonlinear thermal conductivity terms, β, under a given profile area, A_p; the heat transfer first rises and then falls as the fin length increases. From the figure, it shows that the optimum fin length (at which Q/ζ reaches a maximum value) increases as the nonlinear thermal conductivity term, β, increases. It also shows that the optimum value of M can be obtained based upon the value of nonlinear term. Therefore, from the analysis the optimum dimensions of the convection fin with variable thermal conductivity are established and the relative values of optimum M and β are shown in Figure 5.

Figure 6 depicts the effects of multiboiling parameter on the optimum heat transfer rate. For the case of carrying out the optimization of the fin by minimizing the volume of the for the required heat dissipation, Figure 7 shows the effects of multiboiling parameter on the optimum fin dimensions. It is illustrated from the figures that the optimum heat transfer rate and fin length increase with increasing multiboiling

Table 2: Comparison of results.

x(m)	Exact analytical method (˚C)	Finite Element Method (˚C)	Error	% Error
0.000	200.000	200.000	0.000	0.000
0.020	148.133	148.184	0.051	0.034
0.040	113.895	114.031	0.136	0.119
0.060	92.169	92.339	0.170	0.184
0.080	79.725	79.912	0.187	0.235
0.100	74.710	74.880	0.170	0.228

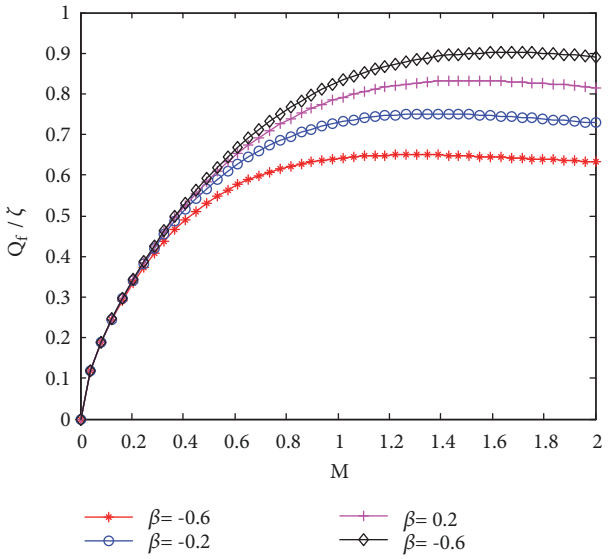

Figure 4: Effects of nonlinear thermal conductivity and thermogeometric parameters on the dimensionless heat transfer, Q_f/ζ.

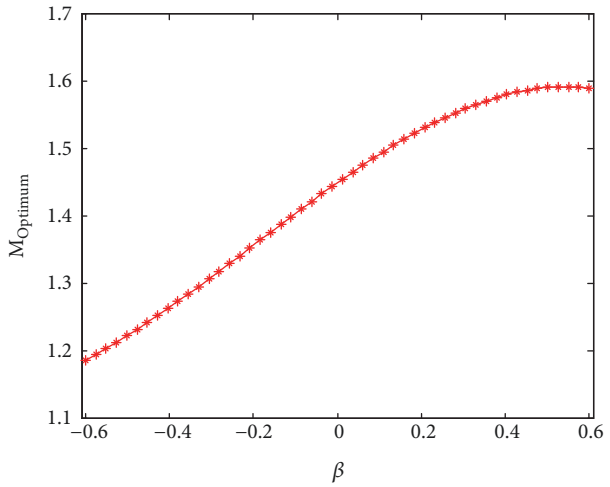

Figure 5: Effects of nonlinear thermal conductivity parameter on the optimum thermogeometric parameter.

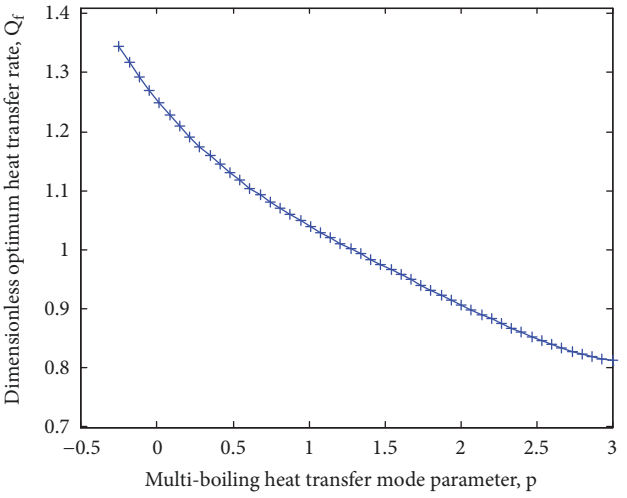

Figure 6: Effects of multiboiling parameter on the optimum heat transfer rate.

heat transfer mode parameter while the optimum fin width decreases with the multiboiling heat transfer mode parameter.

Figure 8 shows the comparison of result of analytical solution and finite element method. Figures 9 and 10 depict temperature-time history at different four points (0.025 m, 0.050m, 0.075 m, and 0.100 m) of the convective-radiative fin with convective and insulated tips, respectively. Figure 11 shows the temperature profile of different heat transfer modes while Figures 12 and 13 show the temperature profiles of the fin at difference times. The temperature histories at the four points decrease at a faster rate initially, slow down thereafter, and finally tend to reach a constant value showing to be near to steady state. Also, a marginal or slightly higher temperature differences are notice between the convective and insulated tip. However, this temperature differences become appreciable as the length of the fin increases and heat is transferred within a short period of time. It could be inferred from the figures and the preceding discussion that, for a short fin that undergo heat transfer for a prolonged period of time, adiabatic/insulted condition at the tip can be assumed without any significant loss in accuracy.

It has been established that the criterion and errors due to one-dimensional heat transfer analysis is that fin base thickness Biot number should be much smaller than unity (precisely, $Bi < 0.1$). To this end, a one-dimensional analysis has been carried out and simulated within $0 < Bi < 0.1$. In this case the error made in the determination of the rate of heat transfer from the fin to the fluid surrounding it is less than 1% [68, 69]. However, when the Biot number is greater than 0.1 (Bi > 0.1), two-dimensional analysis of the

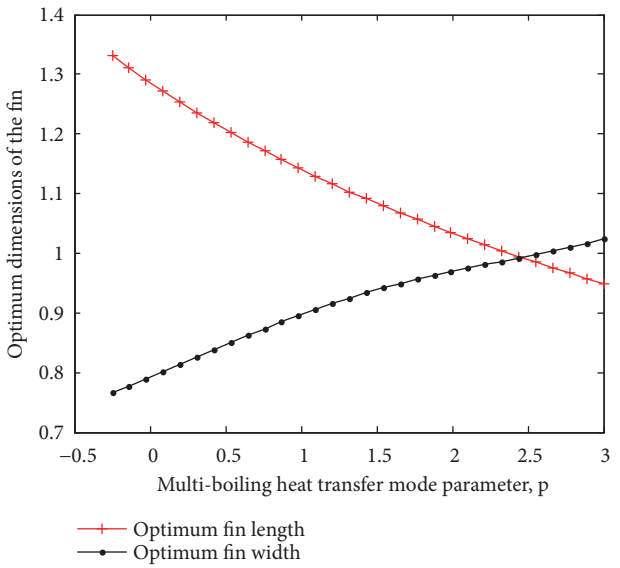

Figure 7: Effects of multiboiling parameter on the optimum fin dimensions.

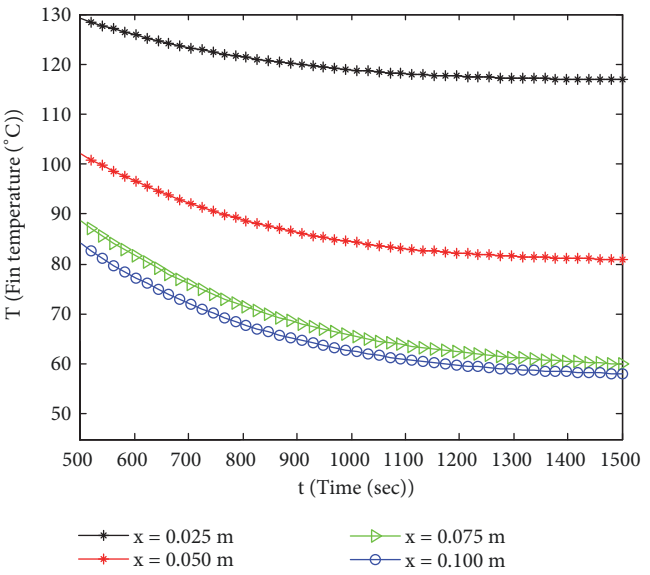

Figure 9: Fin temperature profile at different location (convective tip).

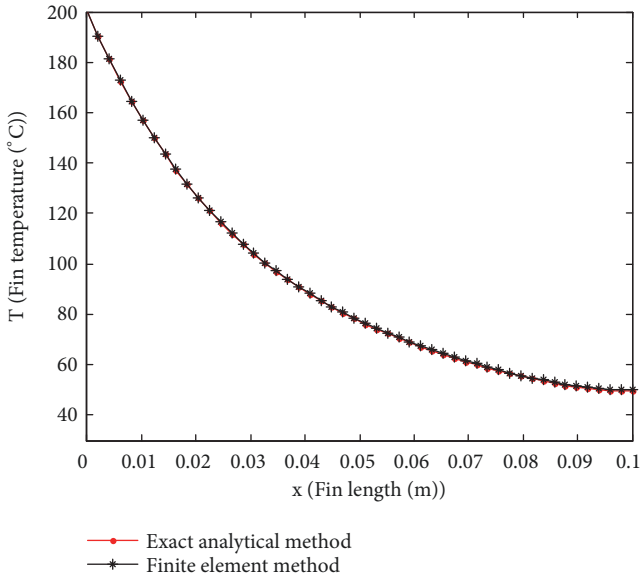

Figure 8: Comparison of results.

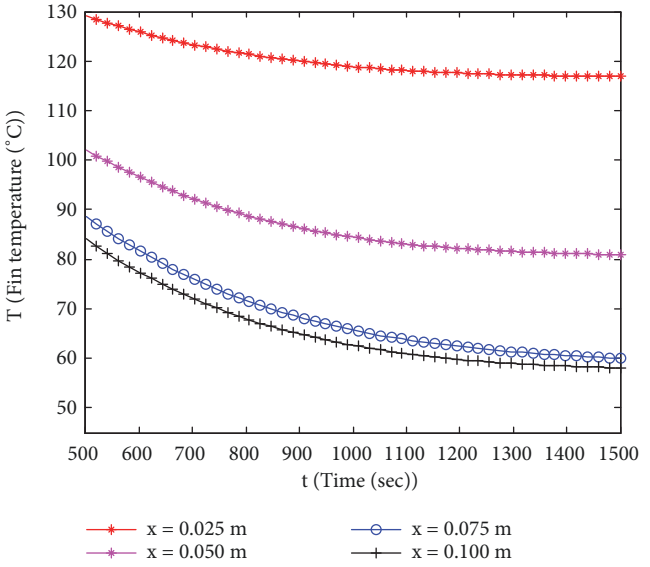

Figure 10: Fin temperature profile at different location (insulated tip).

fin is recommended as one-dimensional analysis predicts unreliable results for such limit.

Figures 14 and 15 show the effects of Biot number (conduction-convection parameter) on the temperature distribution in the fin with convective and insulated tips, respectively. From the figures, it is shown that, as the Biot number increases, the rate of heat transfer through the fin increases as the temperature in the fin drops faster (becomes steeper reflecting high base heat flow rates) as depicted in the figures.

Effects of heat transfer coefficient on the temperature distribution in the fin are shown in Figure 16. It is shown that the temperature profiles for the various heat transfer coefficient coincide initially but part away as we move towards the tip of the fin. This is due to the fact that coefficient of heat transfer coefficient is a factor/multiplier of the temperature difference between the fin surface and surrounding medium ($T\text{-}T_\infty$). It should be noted that the temperature difference between the fin surface and the surrounding decreases as we move away from the fin base to the fin tip despite the increase in the heat transfer coefficient.

It should be noted that, for the fin with heat transfer coefficient which varies according to power law, the hypothetical boundary condition (that is, insulation) at the tip of the fin is taken into account. If the tip is not assumed to be insulated, then the problem becomes overdetermined [69].

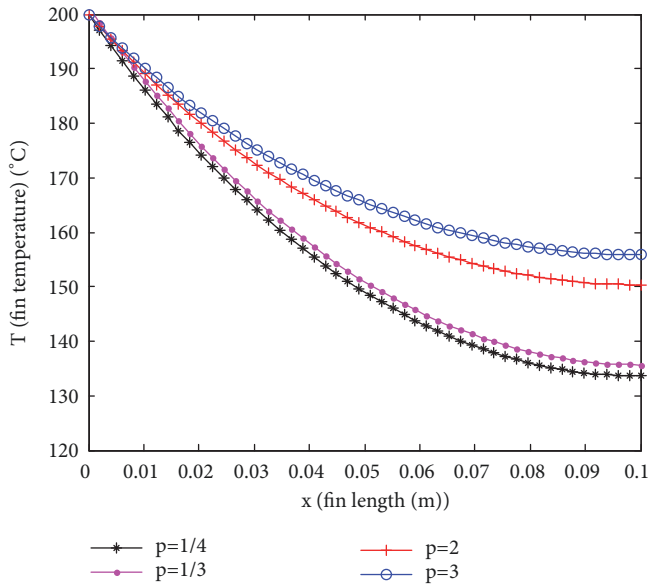

Figure 11: Effects of multiboiling parameter on the fin temperature distribution.

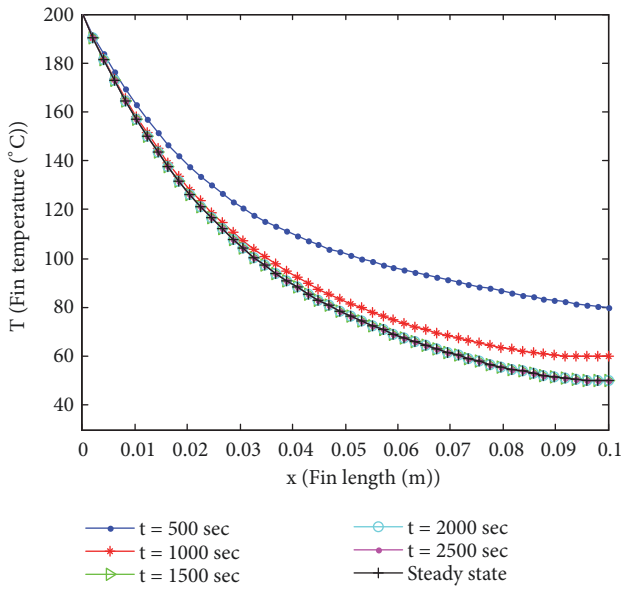

Figure 12: Fin temperature profile at different time (convective tip).

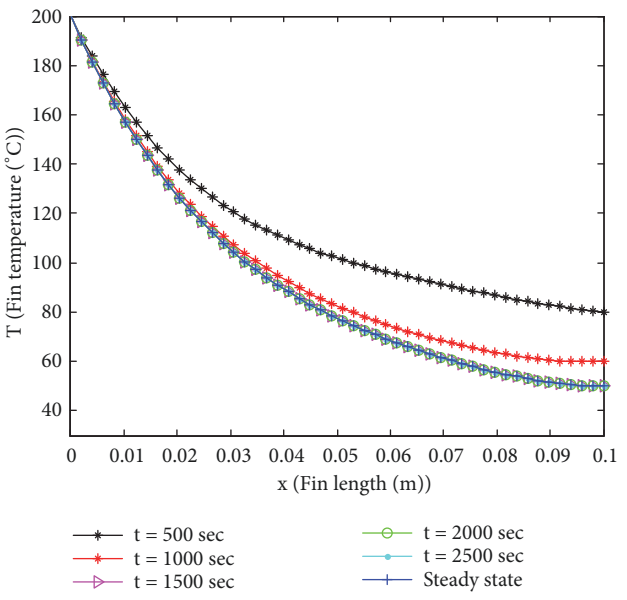

Figure 13: Fin temperature profile at different time (insulated tip).

This boundary condition is realized for sufficiently long fins. Also, it should be stated that the assumption that the heat transfer coefficient is constant yields incorrect.

Figure 17 presents the impact of emissivity on the temperature distribution. The temperature of the fin decreases with increase of emissivity value. This is because of increase of emissive heat by radiation from the fin surface especially when the distance from the base increases. Therefore, heat transfer rate increases as the emissivity increases. The radiative eat transfer can be neglected if the base temperature of the fin is low and the emissivity of the fin surface is near zero. The important things in fins surface must be emissive because high emissivity gives a great amount of heat radiation transfer from the fin [39]. Figure 18 shows effects of magnetic parameter and Hartman number on the temperature distribution in the porous fin. The figure depicts that the induced magnetic field in the fin can improve heat transfer through the fin. It is shown that increase in magnetic field on the fin increases the rate of heat transfer from the fin and consequently improves the efficiency of the fin. Figure 19 shows the effect of thermal conductivity of the fin materials on the thermal response of the fin. It could be inferred from the figure that more heat is transferred from fin made of

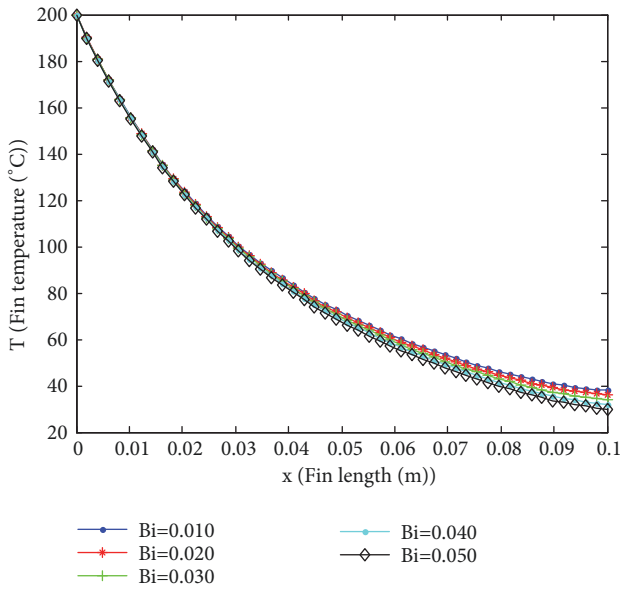

Figure 14: Effects of Biot number on the fin temperature profile (convective tip).

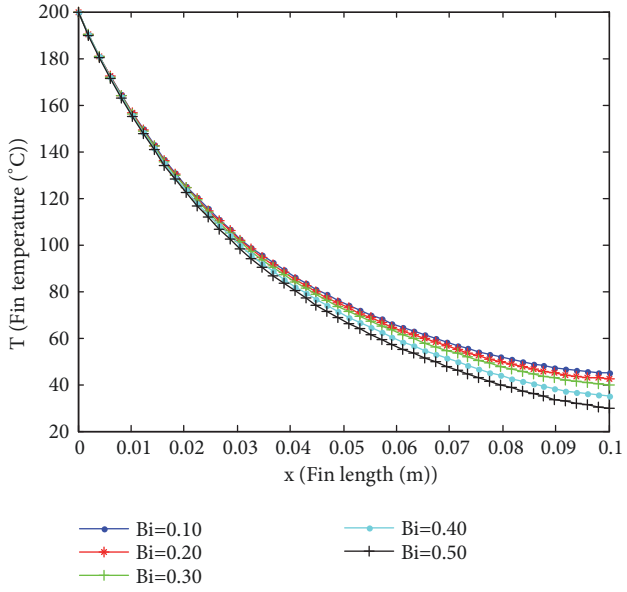

Figure 15: Effects of Biot number on the fin temperature profile (insulated tip).

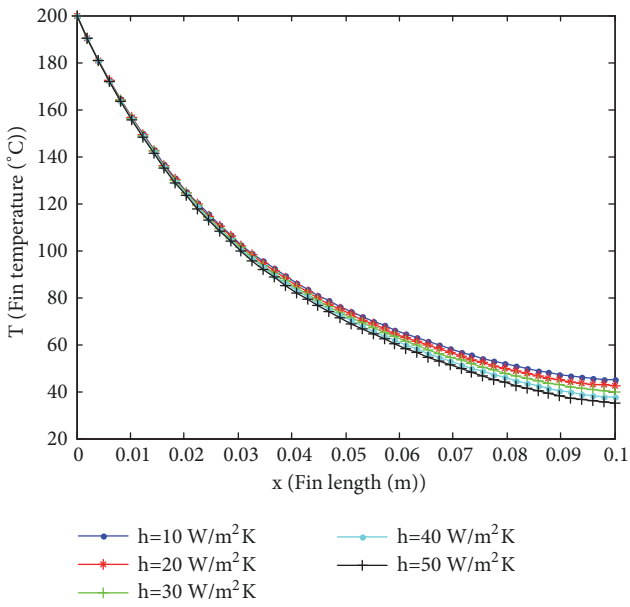

Figure 16: Effects of heat transfer coefficient on the fin temperature profile.

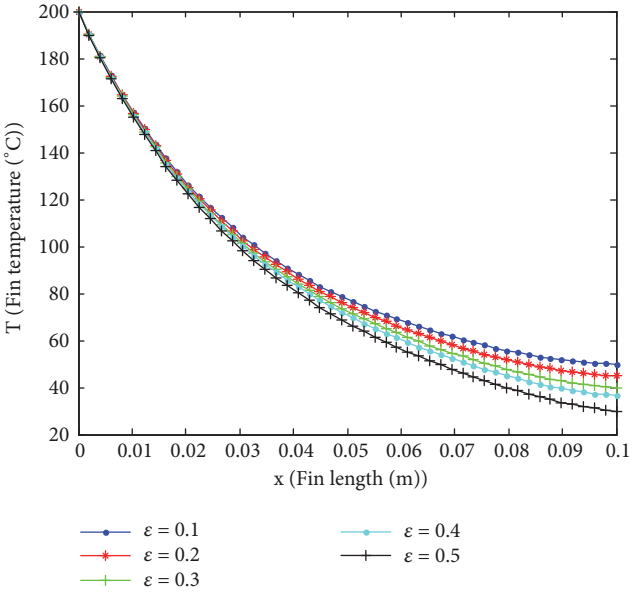

Figure 17: Effects of emissivity on the fin temperature profile.

copper material than the fins made of stainless steel and aluminum materials.

Effects of the thermal and geometric parameters on the temperature profile of the fin are shown in Figure 20 while Figure 21 shows the influence of thermogeometric parameter ($M=(hP/kA)^{0.5}$) on the thermal stability of the fin. It was established that the value of M produces physically unsound behaviour for larger values of the thermogeometric parameter. It is shown that for growing values of the thermogeometric parameter the temperature tends to negative values at the tip of the fin which shows thermal instability, contradicting the assumption of (9). Following the assumptions made regarding the numerical solution of the problem, it was realized that these solutions are not only physically unsound but also point towards thermal instability. Therefore, in order for the solution to be physically sound the fin thermogeometric parameter $M_{\max}$ must not exceed a specific value. By extension in order to ensure stability and avoid numerical diffusion of the solution by the Galerkin finite element method, the thermogeometric parameter must not exceed some certain values for the different multiboiling heat transfer modes.

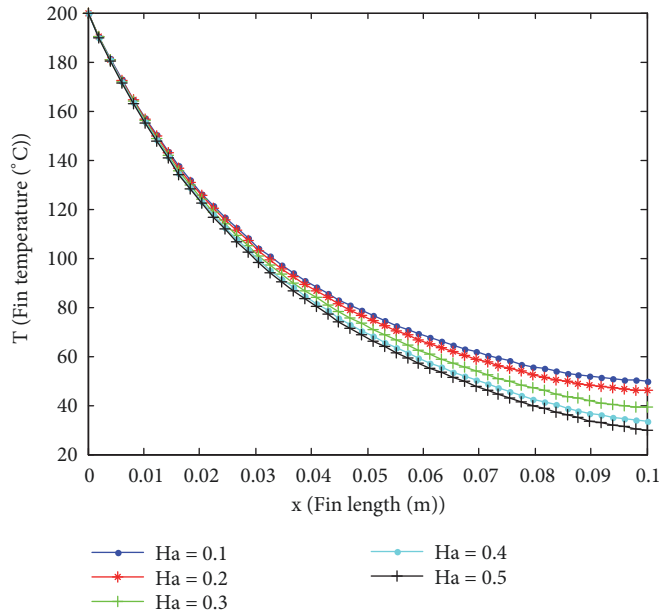

Figure 18: Effects of magnetic parameter on the fin temperature profile.

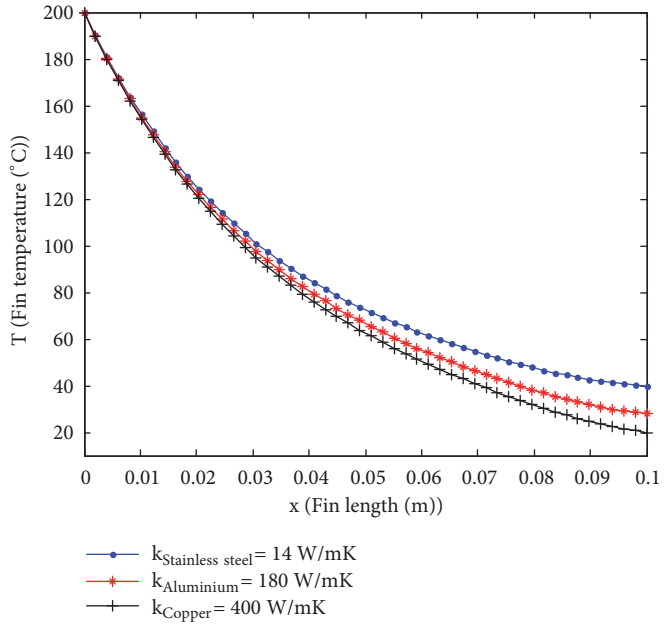

Figure 19: Effects of thermal conductivity on the fin temperature profile.

7. Conclusion

The determination of optimum dimensions and performance of convective-radiative cooling fins subjected to magnetic field has been carried out in this study using finite element method. The numerical solutions were verified by the exact solution for the linearized models using Laplace transform. The optimum dimensions of the convection-radiative fin with variable thermal conductivity were investigated and presented graphically. Also, the effects of other operating parameters on the thermal performance of the fin were investigated using the numerical solutions. The study established that increase in Biot number, convective, radiative, and magnetic parameters, increases the rate of heat transfer from the fin and consequently improves the efficiency of the fin. It is hope that the present study will enhance the understanding of thermal response of solid fin under various factors and fin design considerations.

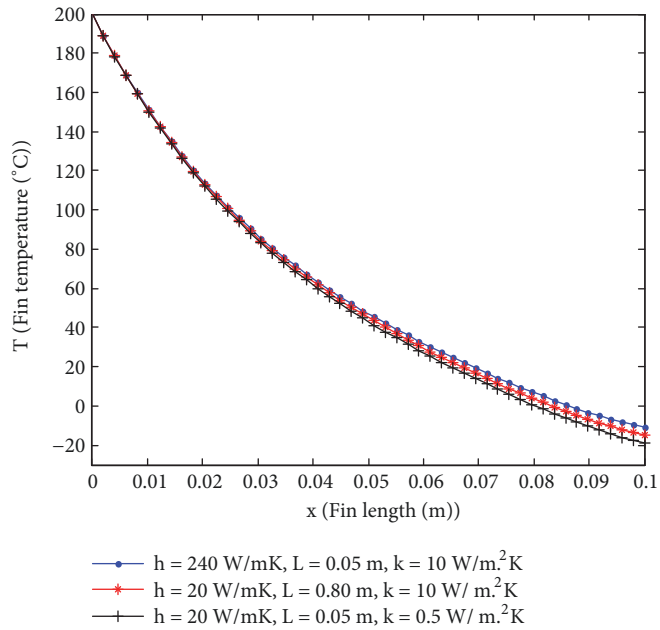

Figure 20: Effects of thermos-geometric parameter on fin temperature profile.

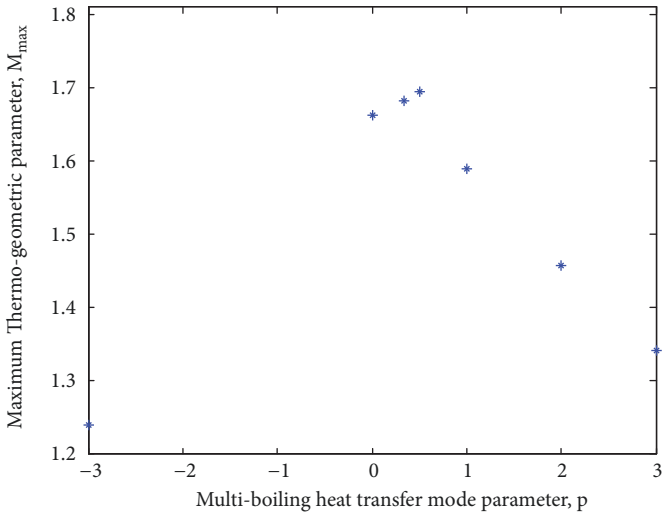

Figure 21: Effects of multiboiling parameter on thermal stability of the fin.

Nomenclature

A_c: Cross-sectional area of the fins, m^2
A_s: Surface area of the fins, m^2
b: Length of the fin
B_o: Magnetic field intensity (T)
c_p: Specific heat (J kg^{-1} K^{-1})
h: Heat transfer coefficient (Jm^{-2} K^{-1})
h_b: Heat transfer coefficient at the base of the fin ($Wm^{-2}k^{-1}$)
J: Total current intensity (A)
Jc: Conduction current intensity (A)
k: Thermal conductivity of the fin material ($Wm^{-1}k^{-1}$)
k_b: Thermal conductivity of the fin material at the base ($Wm^{-1}k^{-1}$)
K: Permeability (m^{-1})
L: Length of the fin (m)
M: Dimensionless thermogeometric parameter
P: Perimeter of the fin (m)
q: Heat transfer rate, W
Qf: Dimensionless optimum fin parameter
δ: Thickness of the fin (m)
t: Time
T: Fin temperature (K)
T_∞: Ambient temperature, K
T_b: Temperature at the base of the fin, K

u: Fluid velocity (m/s)
V: Volume of the fin (m^3)
w: Width of the fin (m)
x: Axial length measured from fin base (m).

Greek Symbols

ε: Emissivity
σ_m: Electric conductivity (A/m)
σst: Stefan–Boltzmann constant ($Wm^2\ K^4$)
ρ: Density of the fluid (kgm^{-3})
β: Thermal conductivity parameter
δ: Thickness of the fin, m
ρ: Density of the fin material (kg/m^3).

Data Availability

The data used in this study are in open literature.

Disclosure

The author declares that the present research did not receive specific funding but was performed as part of the employment of the author in the University of Lagos, Nigeria.

Conflicts of Interest

The author declares that there are no conflicts of interest regarding the publication of this paper.

Acknowledgments

The author expresses sincere appreciation to University of Lagos, Nigeria, for providing material supports and good environment for this work.

References

[1] G. A. Oguntala, R. Abd-Alhameed, and M. G. Sobamowo, "On the effect of magnetic field on thermal performance of convective-radiative fin with temperature-dependent thermal conductivity," *Karbala International Journal of Modern Science*, vol. 4, no. 1, pp. 1–11, 2018..

[2] P. Y. Wang, G. C. Kuo, Y. H. Hu, and W. L. Liaw, "Transient temperature solutions of a cylindrical fin with lateral heat loss," *Wseas Transactions on Mathematics*, vol. 11, no. 10, pp. 918–925, 2012.

[3] R. J. Moitsheki and C. Harley, "Transient heat transfer in longitudinal fins of various profiles with temperature-dependent thermal conductivity and heat transfer coefficient," *Pramana—Journal of Physics*, vol. 77, no. 3, pp. 519–532, 2011.

[4] M. D. Mhlongo and R. J. Moitsheki, "Some exact solutions of nonlinear fin problem for steady heat transfer in longitudinal fin with different profiles," *Advances in Mathematical Physics*, vol. 2014, Article ID 947160, 16 pages, 2014.

[5] S. M. Ali, A. H. Bokhari, and F. D. Zaman, "A lie symmetry classification of a nonlinear fin equation in cylindrical coordinates," *Abstract and Applied Analysis*, vol. 2014, Article ID 527410, 10 pages, 2014.

[6] A. H. Abdel Kader, M. S. Abdel Latif, and H. M. Nour, "General exact solution of the fin problem with variable thermal conductivity," *Propulsion and Power Research*, vol. 5, no. 1, pp. 63–69, 2016.

[7] R. J. Moitsheki and A. Rowjee, "Steady heat transfer through a two-dimensional rectangular straight fin," *Mathematical Problems in Engineering*, vol. 2011, Article ID 826819, 13 pages, 2011.

[8] K. D. Cole, "Computer programs for temperature in fins and slab bodies with the method of Greens functions," *Computer Applications in Engineering Education*, vol. 12, no. 3, pp. 189–197, 2004.

[9] A. Jordan, S. Khaldi, M. Benmouna, and A. Borucki, "Study of non-linear heat transfer problems," *Revue de Physique Appliquée*, vol. 22, pp. 101–105, 1987.

[10] B. Kundu and P. K. Das, "Performance analysis and optimization of straight taper fins with variable heat transfer coefficient," *International Journal of Heat and Mass Transfer*, vol. 45, no. 24, pp. 4739–4751, 2002.

[11] F. Khani, M. A. Raji, and H. H. Nejad, "Analytical solutions and efficiency of the nonlinear fin problem with temperature-dependent thermal conductivity and heat transfer coefficient," *Communications in Nonlinear Science and Numerical Simulation*, vol. 14, no. 8, pp. 3327–3338, 2009.

[12] S. R. Amirkolei and D. D. Ganji, "Thermal performance of a trapezoidal and rectangular profiles fin with temperature-dependent heat transfer coefficient, thermal conductivity and emissivity," *Indian Journal of Scientific Research*, vol. 1, no. 2, pp. 223–229, 2014.

[13] A. Aziz and M. N. Bouaziz, "A least squares method for a longitudinal fin with temperature dependent internal heat generation and thermal conductivity," *Energy Conversion and Management*, vol. 52, no. 8-9, pp. 2876–2882, 2011.

[14] M. G. Sobamowo, "Thermal analysis of longitudinal fin with temperature-dependent properties and internal heat generation using Galerkin's method of weighted residual," *Applied Thermal Engineering*, vol. 99, pp. 1316–1330, 2016.

[15] D. D. Ganji, M. Raghoshay, M. Rahimi, and M. Jafari, "Numerical investigation of fin efficiency and temperature distribution of conductive, convective and radiative straight fins," *International Journal of Recent Research and Applied Studies*, pp. 230–237, 2010.

[16] M. G. Sobamowo, O. M. Kamiyo, and O. A. Adeleye, "Thermal performance analysis of a natural convection porous fin with temperature-dependent thermal conductivity and internal heat generation," *Thermal Science and Engineering Progress*, vol. 1, pp. 39–52, 2017.

[17] M. G. Sobamowo, "Thermal performance and optimum design analysis of fin with variable thermal conductivity using double decomposition method," *Journal of Mechanical Engineering and Technology*, vol. 9, no. 1, pp. 1–32, 2017.

[18] M. G. Sobamowo, L. O. Jayesimi, and J. D. Femi-Oyetoro, "Heat transfer study in a convective-radiative fin with temperature-dependent thermal conductivity and magnetic field using variation of parameter method," *Journal of Applied Mathematics and Computational Mechanics*, vol. 16, no. 3, pp. 85–96, 2017.

[19] A. Moradi and H. Ahmadikia, "Analytical solution for different profiles of fin with temperature- dependent thermal conductivity," *Mathematical Problems in Engineering*, vol. 2010, Article ID 568263, 15 pages, 2010.

[20] S. Sadri, M. R. Raveshi, and S. Amiri, "Efficiency analysis of straight fin with variable heat transfer coefficient and thermal

conductivity," *Journal of Mechanical Science and Technology*, vol. 26, no. 4, pp. 1283–1290, 2012.

[21] P. L. Ndlovu and R. J. Moitsheki, "Analytical solutions for steady heat transfer in longitudinal fins with temperature-dependent properties," *Mathematical Problems in Engineering*, vol. 2013, Article ID 273052, 14 pages, 2013.

[22] S. Mosayebidorcheh, D. D. Ganji, and M. Farzinpoor, "Approximate solution of the nonlinear heat transfer equation of a fin with the power-law temperature-dependent thermal conductivity and heat transfer coefficient," *Propulsion and Power Research*, vol. 3, no. 1, pp. 41–47, 2014.

[23] S. E. Ghasemi, M. Hatami, and D. D. Ganji, "Thermal analysis of convective fin with temperature-dependent thermal conductivity and heat generation," *Case Studies in Thermal Engineering*, vol. 4, pp. 1–8, 2014.

[24] D. D. Ganji and A. S. Dogonchi, "Analytical investigation of convective heat transfer of a longitudinal fin with temperature-dependent thermal conductivity, heat transfer coefficient and heat generation," *International Journal of Physical Sciences*, vol. 9, no. 21, pp. 466–474, 2014.

[25] M. G. Sobamowo, O. A. Adeleye, and A. A. Yinusa, "Analysis of convective-radiative porous fin with temperature-dependent internal heat generation and magnetic using homotopy perturbation method," *Journal of Computational and Applied Mechanics*, vol. 12, no. 2, pp. 127–145, 2017.

[26] C. Arslantürk, "Optimization of straight fins with a step change in thickness and variable thermal conductivity by homotopy perturbation method," *Journal of Thermal Science and Technology*, vol. 30, no. 2, pp. 9–19, 2010.

[27] D. D. Ganji, Z. Z. Ganji, and H. D. Ganji, "Determination of temperature distribution for annular fins with temperature dependent thermal conductivity by HPM," *Thermal Science*, vol. 15, no. 1, pp. S111–S115, 2011.

[28] H. A. Hoshyar, I. Rahimipetroudi, D. D. Ganji, and A. R. Majidian, "Thermal performance of porous fins with temperature-dependent heat generation via the homotopy perturbation method and collocation method," *Journal of Applied Mathematics and Computational Mechanics*, vol. 14, no. 4, pp. 53–65, 2015.

[29] I. V. Singh, K. Sandeep, and R. Prakash, "Heat transfer analysis of two-dimensional fins using a meshless element free Galerkin method," *Numerical Heat Transfer, Part A: Applications*, vol. 44, no. 1, pp. 73–84, 2003.

[30] S. Basri, M. M. Fakir, F. Mustapha et al., "Heat distribution in rectangular fins using efficient finite element and differential quadrature methods," *Engineering*, vol. 1, pp. 151–160, 2009.

[31] T. Singh, S. Shrivastava, and H. S. Ber, "Analysis of unsteady heat conduction through short fin with applicability of quasi theory," *International Journal of Mechanical Engineering and Robotics Research*, vol. 2, no. 1, pp. 269–283, 2013.

[32] A. K. Sao and Y. P. Banjare, "Analysis of thermal characteristics of transient heat conduction through long fin and comparison with exact fin theory and quasi steady theory," *International Journal of Emerging Technology and Advanced Engineering*, vol. 4, no. 11, pp. 157–166, 2014.

[33] B. Lotfi and A. Belkacem, "Numerical method for optimum performance of fin profiles," *International Journal of Current Engineering and Technology*, vol. 6, no. 4, pp. 3990–3998, 2014.

[34] A. A. A. A. Al-Rashed, L. Kolsi, H. F. Oztop, N. Abu-Hamdeh, and M. N. Borjini, "Natural convection and entropy production in a cubic cavity heated via pin-fins heat sinks," *International Journal of Heat and Technology*, vol. 35, no. 1, pp. 109–115, 2017.

[35] D. Taler and J. Taler, "Steady-state and transient heat transfer through fins of complex geometry," *Archives of Thermodynamics*, vol. 35, no. 2, pp. 117–133, 2014.

[36] P. Malekzadeh and H. Rahideh, "Two-dimensional nonlinear transient heat transfer analysis of variable section pin fins," *Energy Conversion and Management*, vol. 50, no. 4, pp. 916–922, 2009.

[37] C. S. Reddy, Y. R. Reddy, and P. Srikanth, "Application of B–spline based FEM to one-dimensional problems," *International Journal of Current Engineering and Technology*, vol. 3, pp. 137–140, 2014.

[38] Y. Sun, J. Ma, B. Li, and Z. Guo, "Predication of nonlinear heat transfer in a convective-radiative fin with temperature-dependent properties by the collocation spectral method," *Numerical Heat Transfer, Part B: Fundamentals*, vol. 69, no. 1, pp. 8–73, 2016.

[39] G. Rajul, T. Harishchandra, and T. Brajesh, "Nonlinear numerical analysis of convective-radiative fin using MLPG method," *International Journal of Heat and Technology*, vol. 35, no. 4, pp. 721–729, 2017.

[40] Z. Wei, L. Haifang, D. Xiaoze et al., "Numerical and experimental research on performance of single-row finned tubes in air-cooled power plants," *International Journal of Heat and Technology*, vol. 34, no. 1, pp. 137–142, 2016.

[41] F. Hajabdollahi, H. H. Rafsanjani, Z. Hajabdollahi, and Y. Hamidi, "Multi-objective optimization of pin fin to determine the optimal fin geometry using genetic algorithm," *Applied Mathematical Modelling*, vol. 36, no. 1, pp. 244–254, 2012.

[42] H. Fatoorehchi and H. Abolghasemi, "Investigation of nonlinear problems of heat conduction in tapered cooling fins via symbolic programming," *Applications & Applied Mathematics*, vol. 7, no. 2, pp. 717–734, 2012.

[43] M. S. A. Latif, A. H. A Kader, and H. M. Nour, "Exact implicit solution of nonlinear heat transfer in rectangular straight fin using symmetry reduction methods," *Applications & Applied Mathematics*, vol. 10, no. 2, pp. 864–877, 2015.

[44] A. Mahmoudi and I. Mejri, "Analysis of conduction-radiation heat transfer with variable thermal conductivity and variable refractive index: Application of the lattice Boltzmann method," *International Journal of Heat and Technology*, vol. 33, no. 1, pp. 1–8, 2015.

[45] M. G. Sobamowo, "Analysis of convective longitudinal fin with temperature-dependent thermal conductivity and internal heat generation," *Alexandria Engineering Journal*, vol. 56, no. 1, pp. 1–11, 2017.

[46] M. G. Sobamowo, B. Y. Ogumola, and G. Nzebuka, "Finite volume method for analysis of convective longitudinal fin with temperature-dependent thermal conductivity and internal heat generation," *Defect and Diffusin Forum*, vol. 374, pp. 106–120, 2017.

[47] M. G. Sobamowo, G. A. Oguntala, and J. D. Femi-Oyetoro, "Investigation of the effects of magnetic field on the thermal performance of convective-radiative fin using wavelet collocation method," *Annals of Faculty of Engineering Honedoara-International Journal of Engineering. Tome XV*, pp. 179–186, 2017.

[48] M. G. Sobamowo, "Heat transfer study in porous fin with temperature-dependent thermal conductivity and internal heat generation using Legendre wavelet collocation method," *Communication in Mathematical Modeling and Applications*, vol. 2, no. 3, pp. 16–28, 2017.

[49] G. M. Sobamowo and O. M. Kamiyo, "Multi-boiling heat transfer analysis of a convective straight fin with temperature-dependent thermal properties and internal heat generation," *Journal of Applied and Computational Mechanics*, vol. 3, no. 4, pp. 229–239, 2017.

[50] M. G. Sobamowo, "Analysis of heat transfer in porous fin with temperature-dependent thermal conductivity and internal heat generation using Chebychev spectral collocation method," *Journal of Computational Applied Mechanics*, vol. 48, no. 2, pp. 271–287, 2017.

[51] A. J. Chapman, "Transient heat conduction in annular fins of uniform thickness," in *Proceedings of the Chemical Engineering Symposium*, vol. 55, no. 29, pp. 195–201, 1959.

[52] A. B. Donaldson and A. R. Shouman, "Unsteady-state temperature distribution in a convecting fin of constant area," *Applied Scientific Research*, vol. 26, no. 1-2, pp. 75–85, 1972.

[53] N. V. Suryanarayana, "Transient response of straight fins," *Journal of Heat Transfer*, vol. 97, no. 3, pp. 417–423, 1975.

[54] N. V. Suryanarayana, "Transient response of straight fins part II," *Journal of Heat Transfer*, vol. 98, no. 2, pp. 324–326, 1976.

[55] J. Mao and S. Rooke, "Transient analysis of extended surfaces with convective tip," *International Communications in Heat and Mass Transfer*, vol. 21, no. 1, pp. 85–94, 1994.

[56] J. V. Beck, K. D. Cole, A. Haji-Sheikh, and B. Litkouhi, *Heat Conduction Using Green's Functions Hemisphere, New York*, 1992.

[57] R. H. Kim, "The Kantorovich method in the variational formulation to an unsteady heat conduction," *Letters in Heat and Mass Transfer*, vol. 3, no. 1, pp. 73–80, 1976.

[58] A. Aziz and T. Y. Na, "Transient response of fins by coordinate perturbation expansion," *International Journal of Heat and Mass Transfer*, vol. 23, no. 12, pp. 1695–1698, 1980.

[59] A. Aziz and A. D. Kraus, "Transient heat transfer in extended surfaces," *Applied Mechanics Reviews*, vol. 48, no. 3, pp. 317–349, 1995.

[60] A. Campo and A. Salazar, "Similarity between unsteady-state conduction in a planar slab for short times and steady-state conduction in a uniform, straight fin," *Heat and Mass Transfer*, vol. 31, no. 5, pp. 365–370, 1996.

[61] A. K. Saha and S. Acharya, "Parametric study of unsteady flow and heat transfer in a pin-fin heat exchanger," *International Journal of Heat and Mass Transfer*, vol. 46, no. 20, pp. 3815–3830, 2003.

[62] T. H. Hsu and C. K. Chen, "Transient analysis of combined forced and free convection conduction along a vertical circular fin in micro polar fluids," *Numerical Heat Transfer, Part A: Applications*, vol. 19, no. 2, pp. 177–185, 1991.

[63] M. Benmadda and M. Lacroix, "Transient natural convection from a finned surface for thermal storage in an enclosure," *Numerical Heat Transfer, Part A: Applications*, vol. 29, no. 1, pp. 103–114, 1996.

[64] D. K. Tafti, L. W. Zhang, and G. Wang, "Time-dependent calculation procedure for fully developed and developing flow and heat transfer in louvered fin geometries," *Numerical Heat Transfer, Part A: Applications*, vol. 35, no. 3, pp. 225–249, 1999.

[65] A. K. Saha and S. Acharya, "Unsteady simulation of turbulent flow and heat transfer in a channel with periodic array of cubic pin-fins," *Numerical Heat Transfer, Part A: Applications*, vol. 46, no. 8, pp. 731–763, 2004, Exact Solution for Transient Heat Conduction through Long Fin.

[66] M. Tutar and A. Akkoca, "Numerical analysis of fluid flow and heat transfer characteristics in three-dimensional plate fin-and-tube heat exchangers," *Numerical Heat Transfer, Part A: Applications*, vol. 46, no. 3, pp. 301–321, 2004.

[67] I. Mutlu and T. T. Al-Shemmeri, "Steady-state and transient performance of a shrouded longitudinal fin array," *International Communications in Heat and Mass Transfer*, vol. 20, no. 1, pp. 133–143, 1993.

[68] R. K. Irey, "Errors in the one-dimensional fin solution," *Journal of Heat Transfer*, vol. 90, pp. 175-176, 1968.

[69] K. Laor and H. Kalman, "The effect of tip convection on the performance and optimum dimensions of cooling fins," *International Communications in Heat and Mass Transfer*, vol. 19, no. 4, pp. 569–584, 1992.

[70] W. Lau and C. W. Tan, "Errors in one-dimensional heat transfer analysis in straight and annular fins," *Journal of Heat Transfer*, vol. 95, no. 4, pp. 549–551, 1973.

[71] H. C. Unal, "Determination of the temperature distribution in an extended surface with a non-uniform heat Effect of the boundary condition at a fin tip on the performance of the fin 1495 transfer coefficient," *International Journal of Heat and Mass Transfer*, vol. 28, pp. 2279–2284, 1985.

[72] M. G. Sobamowo and A. A. Oyediran, "Effects of Thermo-geometric parameter on the heat transfer rate in Straight fin wit variable thermal conductivity," A Festschrift Celebrating 70 years of Life and Excellence of Emeritus Professor Vincent Olusegun Sowemimo Olunloyo, 2013.

[73] A. N. Hrymak, G. J. McRae, and A. W. Westerberg, "Combined analysis and optimization of extended heat transfer surfaces," *ASME Journal of Heat Transfer*, vol. 107, p. 527, 1985.

[74] A. Sonn and A. Bar-Cohen, "Optimum cylindrical pin fin," *ASME Journal of Heat Transfer*, vol. 103, no. 4, pp. 814-815, 1981.

[75] P. Razelos and K. Imre, "Minimum mass convective fins with variable heat transfer coefficients," *Journal of The Franklin Institute*, vol. 315, no. 4, pp. 269–282, 1983.

[76] P. Razelos and K. Imre, "The optimum dimensions of circular fins with variable thermal parameters," *ASME Journal of Heat Transfer*, vol. 102, no. 3, pp. 420–425, 1980.

[77] R. Pitchumani and U. V. Shenoy, "A unified approach to determining optimum shapes for cooling fins of various geometries," *Private Communication*, 1988.

[78] Bhargava and R. J. Duffin, "On the non-linear method of Wilkins for cooling fin optimization," *SfAM Journal of Applied Mathematics*, vol. 24, p. 441, 1973.

[79] I. E. Wilkins Jr., "Minimum mass thin fins which transfer heat only by radiation to surroundings at absolute zero," *Journal of the Society for Industrial and Applied Mathematics*, vol. 8, p. 630, 1960.

[80] P. Razelos, "The optimum dimensions of convective pin fins with internal heat generation," *Journal of The Franklin Institute*, vol. 321, no. 1, pp. 1–19, 1986.

[81] C. J. Maday, "The minimum weight one-dimensional straight fin," *ASME Journal of Engineering for Industry*, vol. 96, no. 1974, p. 161, 1974.

[82] K. Laor and H. Kalman, "Performance and optimum dimensions of different cooling fins with a temperature-dependent heat transfer coefficient," *International Journal of Heat and Mass Transfer*, vol. 39, no. 9, pp. 1993–2003, 1996.

[83] A. Taklifi, C. Aghanajafi, and H. Akrami, "The Effect of MHD on a Porous Fin Attached to a Vertical Isothermal Surface," *Transport in Porous Media*, vol. 85, no. 1, pp. 215–231, 2010.

[84] S. Rezazadeh Amirkolaei, D. D. Ganji, and H. Salarian, "Determination of temperature distribution for porous fin which is exposed to uniform magnetic field to a vertical isothermal surface by homotopy analysis method and collocation method," *Indian Journal of Scientific Research*, vol. 1, no. 2, pp. 215–222, 2014.

[85] H. A. Hoshyar, D. D. Ganji, and A. R. Majidian, "Least square method for porous fin in the presence of uniform magnetic field," *Journal of Applied Fluid Mechanics*, vol. 9, no. 2, pp. 661–668, 2016.

[86] M. G. Sobamowo and A. O. Adesina, "Thermal performance analysis of convective-radiative fin with temperature-dependent thermal conductivity in the presence of uniform magnetic field using partial noether method," *Journal of Thermal Engineering*, vol. 4, no. 5, pp. 2287–2302, 2018.

[87] J. Ma, Y. Sun, and B. Li, "Spectral collocation method for transient thermal analysis of coupled conductive, convective and radiative heat transfer in the moving plate with temperature dependent properties and heat generation," *International Journal of Heat and Mass Transfer*, vol. 114, pp. 469–482, 2017.

[88] J. Ma, Y. Sun, and B. Li, "Simulation of combined conductive, convective and radiative heat transfer in moving irregular porous fins by spectral element method," *International Journal of Thermal Sciences*, vol. 118, pp. 475–487, 2017.

[89] H. Chen, J. Ma, and H. Liu, "Least square spectral collocation method for nonlinear heat transfer in moving porous plate with convective and radiative boundary conditions," *International Journal of Thermal Sciences*, vol. 132, pp. 335–343, 2018.